

Supplementary Information: Energetic Costs, Precision, and Transport Efficiency of Molecular Motors

Wonseok Hwang¹ and Changbong Hyeon^{1,*}

¹*Korea Institute for Advanced Study, Seoul 02455, Korea*

CONTENTS

Calculation of V and D of kinesin-1 in 6-state multi-cyclic model	1
Master equation	1
Generating function	2
Generating function at the asymptotic limit	2
Velocity and Diffusion coefficient	3
Characteristic polynomial	3
Explicit expression of $J_{\mathcal{F}}$	4
Analysis of other types of kinesins	4
Kinesin-1 mutant (Kin6AA)	4
Kinesin-2 (KIF17, KIF3AB)	4
Myosin-V	4
Calculation of V and D	5
Affinities and heat production	5
Dynein	6
Affinity and heat production	6
F ₁ -ATPase	6
V , D , affinities, and heat production	7
Unicyclic kinetic model for kinesin-1	7
Unicyclic kinetic model for myosin-V	7
The lower bound of \mathcal{Q} for unicyclic model	7
References	7

CALCULATION OF V AND D OF KINESIN-1 IN 6-STATE MULTI-CYCLIC MODEL

To obtain the expression of V and D for multicyclic kinetic network model in terms of a set of rate constants $\{k_{ij}\}$, we have generalized the technique by Koza [1] (Alternatively, technique based on the large deviation theory can be used. See Ref. [2, 3]). We

define the generating functions for the given network model.

In the 6-state double-cycle kinetic network (Fig. 1A), we define the three distinct generating functions for \mathcal{F} , \mathcal{B} , and \mathcal{X} cycles. The two generating functions for the subcycles, \mathcal{F} and \mathcal{B} -cycles, are convenient to calculate the chemical current $J_{\mathcal{F}}$ and $J_{\mathcal{B}}$ in each sub-cycle. To calculate V and D in a convenient way, we have defined another generating function for \mathcal{X} -cycle, which is not explicit in the kinetic scheme in Fig. 1A. The \mathcal{X} -cycle differs from \mathcal{F} , \mathcal{B} -cycle in that the former explicitly considers the physical location of the motor along the 1D track. Although V is obtained either evaluating $V = d_0(J_{\mathcal{F}} - J_{\mathcal{B}})$ or $V = d_0 J_{\mathcal{X}}$, it is not straightforward to decompose the diffusivity of motor D into the contributions from \mathcal{F} and \mathcal{B} -cycle.

The expressions of $J_{\mathcal{F}}(\{k_{ij}\})$, $J_{\mathcal{B}}(\{k_{ij}\})$, $V(\{k_{ij}\})$ and $D(\{k_{ij}\})$ can be obtained by considering an asymptotic limit ($t \rightarrow \infty$) of the corresponding generating function.

In what follows, we provide the derivation of generating function in details. In order to derive the generating function, we introduce a generalized index for reaction cycle \mathcal{I} , with $\mathcal{I} = \mathcal{F}$, \mathcal{B} , or \mathcal{X} .

Master equation

For a system with N chemical states ($\{1, 2, \dots, N\}$), a generalized state $\mu^{\mathcal{I}}(t)$ is defined by using the chemical state of the motor at time t and the number of completed \mathcal{I} -cycles ($n_c^{\mathcal{I}}(t)$). For kinesins whose dynamics can be mapped onto the 6-state double-cycle kinetic network model, if the motor is in the i -th chemical state ($i \in \{1, 2, \dots, N\}$ with $N = 6$) at time t , the generalized state of the motor in the \mathcal{I} -cycle is $\mu^{\mathcal{I}}(t) = i + N \times n_c^{\mathcal{I}}(t)$, where \mathcal{I} could denote either \mathcal{F} , \mathcal{B} , or \mathcal{X} depending on reader's interest. $P(\mu^{\mathcal{I}}, t)$ that represents the probability of the system being in $\mu^{\mathcal{I}}$ at time t , satisfies

$$\frac{\partial P(\mu^{\mathcal{I}}, t)}{\partial t} = \sum_{\xi} K_{\mu^{\mathcal{I}} - \xi, \mu^{\mathcal{I}}} P(\mu^{\mathcal{I}} - \xi, t) - K_{\mu^{\mathcal{I}}, \mu^{\mathcal{I}} - \xi} P(\mu^{\mathcal{I}}, t), \quad (\text{S1})$$

where $K_{\mu,\nu} = \sum_{\alpha} k_{\mu,\nu}^{\alpha}$ and k_{ij}^{α} denotes the rate of transition from state i to state j that follows the α -th pathway. Here, the periodicity of network model imposes $k_{\mu+N,\nu+N}^{\alpha} = k_{\mu,\nu}^{\alpha}$, $K_{\nu+N,\mu+N} = K_{\nu,\mu}$, and $k_{\mu,\nu}^{\alpha} = k_{i,j}^{\alpha}$ for $\mu = i \pmod{N}$ and $\nu = j \pmod{N}$. The range of (integer) summation index ξ depends on the existing pathways for \mathcal{I} -cycle. Hereafter, the superscript \mathcal{I} on μ shall be omitted for simplicity.

Following Ref. [1], we define

$$P_j(\mu, t) \equiv P(\mu, t) \delta_{\mu,j}^N \quad (\text{S2})$$

where,

$$\delta_{\mu,j}^N = \begin{cases} 1, & \text{if } j = \mu \pmod{N} \\ 0, & \text{otherwise} \end{cases} \quad (\text{S3})$$

Here, $j \in \{1, 2, \dots, N\}$. Multiplying $\delta_{\mu,j}^N$ on both sides of Eq.S1 and using the equality $\delta_{\mu,j}^N = \delta_{\mu-\xi,j-\xi}^N$, we get

$$\frac{\partial P_j(\mu, t)}{\partial t} = \sum_{\xi} K_{j-\xi,j} P_{j-\xi}(\mu - \xi, t) - K_{j,j-\xi} P_j(\mu, t). \quad (\text{S4})$$

Generating function

We define a generating function to derive V and D . The generating function for \mathcal{I} -cycle is defined by

$$\mathcal{G}_j^{\mathcal{I}}(z, t) \equiv \sum_{\mu=-\infty}^{\infty} e^{zX_{\mu}^{\mathcal{I}}} P_j(\mu, t). \quad (\text{S5})$$

where $X_{\mu}^{\mathcal{I}}$ denotes the generalized coordinate for \mathcal{I} -cycle at generalized state μ . Then Eq.(S4) and the equality $(X_{\mu}^{\mathcal{I}} - X_{\mu-\xi}^{\mathcal{I}})P_{j-\xi}(\mu - \xi, t) = (X_j^{\mathcal{I}} - X_{j-\xi}^{\mathcal{I}})P_{j-\xi}(\mu - \xi, t)$ with $\delta_{\mu,j}^N = \delta_{\mu-\xi,j-\xi}^N$ lead to

$$\begin{aligned} \frac{\partial \mathcal{G}_j^{\mathcal{I}}(z, t)}{\partial t} &= \sum_{\xi} \left(\sum_{\mu=-\infty}^{\infty} e^{zX_{\mu}^{\mathcal{I}}} K_{j-\xi,j} P_{j-\xi}(\mu - \xi, t) \right) - \sum_{\xi} K_{j,j-\xi} \mathcal{G}_j^{\mathcal{I}}(z, t) \\ &= \sum_{\xi} e^{z d_{j-\xi,j}^{\mathcal{I}}} K_{j-\xi,j} \mathcal{G}_{j-\xi}^{\mathcal{I}}(z, t) - \sum_{\xi} K_{j,j-\xi} \mathcal{G}_j^{\mathcal{I}}(z, t) \end{aligned} \quad (\text{S6})$$

where $d_{\mu\nu}^{\mathcal{I}} \equiv X_{\nu}^{\mathcal{I}} - X_{\mu}^{\mathcal{I}}$. In general, different cycle has different $\{d_{\mu,\nu}^{\mathcal{I}}\}$. For example, for the \mathcal{F} -cycle in Fig. 1A,

$$d_{i,j}^{\mathcal{F}} = \begin{cases} 1, & \text{for } i = 6, j = 1 \\ -1, & \text{for } i = 1, j = 6 \\ 0, & \text{otherwise,} \end{cases} \quad (\text{S7})$$

for the \mathcal{B} -cycle,

$$d_{i,j}^{\mathcal{B}} = \begin{cases} 1, & \text{for } i = 3, j = 4 \\ -1, & \text{for } i = 4, j = 3 \\ 0, & \text{otherwise,} \end{cases} \quad (\text{S8})$$

and for the \mathcal{X} -cycle,

$$d_{i,j}^{\mathcal{X}} = \begin{cases} 1, & \text{for } i = 2, j = 5 \\ -1, & \text{for } i = 5, j = 2 \\ 0, & \text{otherwise.} \end{cases} \quad (\text{S9})$$

In fact, Eq. (S6) can be expressed more succinctly as

$$\partial_t \mathcal{G}_j^{\mathcal{I}}(z, t) = \sum_{i=1}^N \Gamma_{ij}^{\mathcal{I}} \mathcal{G}_i^{\mathcal{I}}(z, t) \quad (\text{S10})$$

where

$$\Gamma_{ij}^{\mathcal{I}}(z) = \begin{cases} \sum_{\alpha} k_{ij}^{\alpha} e^{z d_{ij}^{\mathcal{I},\alpha}}, & \text{if } i \neq j \\ -\sum_{m=1(\neq i)}^N \sum_{\alpha} k_{im}^{\alpha}, & \text{if } i = j \end{cases} \quad (\text{S11})$$

With α , an index to discern the pathways, Γ can be written in the form of $N \times N$ matrix.

Generating function at the asymptotic limit

Here we consider the asymptotic limit ($t \rightarrow \infty$) in which V and D are well defined for an arbitrary chemical network model. The general solution of Eq.(S10)

can be written as [1]

$$\mathcal{G}_j^{\mathcal{I}}(z, t) = \sum_m T_{mj}^{\mathcal{I}}(z, t) e^{\lambda_m^{\mathcal{I}}(z)t} \quad (\text{S12})$$

where $\lambda_m^{\mathcal{I}}(z)$'s ($m = 0, 1, 2, \dots, N$) are the eigenvalues of $\Gamma^{\mathcal{I}}(z)$. For a system in (unique) steady state, the eigenvalues satisfy $\lambda_0^{\mathcal{I}}(0) = 0$ and $\lambda_m^{\mathcal{I}}(0) < 0$ for $m \neq 0$. Thus, at $t \rightarrow \infty$ and when $z \sim 0$,

$$\lim_{t \rightarrow \infty} \mathcal{G}_j^{\mathcal{I}}(z, t) \sim T_{0j}^{\mathcal{I}}(z, t) e^{\lambda_0^{\mathcal{I}}(z)t} \quad (\text{S13})$$

Now, summed over the index j , Eq.(S5) is led to

$$\begin{aligned} \sum_{j=1}^N \mathcal{G}_j^{\mathcal{I}}(z, t) &= \sum_{j=1}^N \sum_{\mu=-\infty}^{\infty} e^{zX_{\mu}^{\mathcal{I}}} P_j(\mu, t) \\ &= \sum_{\mu=-\infty}^{\infty} e^{zX_{\mu}^{\mathcal{I}}} P(\mu, t) \\ &\equiv \mathcal{G}^{\mathcal{I}}(z, t). \end{aligned} \quad (\text{S14})$$

From Eq.(S13), at $t \rightarrow \infty$, we have

$$\mathcal{G}^{\mathcal{I}}(z, t) \sim \sum_j T_{0j}^{\mathcal{I}}(z, t) e^{\lambda_0^{\mathcal{I}}(z)t} = h^{\mathcal{I}}(z, t) e^{\lambda_0^{\mathcal{I}}(z)t} \quad (\text{S15})$$

where $h^{\mathcal{I}}(z, t) \equiv \sum_j T_{0j}^{\mathcal{I}}(z, t)$. Since $\mathcal{G}^{\mathcal{I}}(0, t) = 1$ and $\lambda_0^{\mathcal{I}}(z=0) = 0$, $h^{\mathcal{I}}(0, t) \sim 1$ at $t \rightarrow \infty$.

Velocity and Diffusion coefficient

In this section, we first define the flux $J^{\mathcal{I}}$ and the diffusion coefficient $D^{\mathcal{I}}$ of \mathcal{I} -cycle using $X^{\mathcal{I}}(t)$ at $t \rightarrow \infty$. Then by using the asymptotic form of the generating function, we will get the relation between $J^{\mathcal{I}}$ and $D^{\mathcal{I}}$, and the lowest eigenvalue $\lambda_0^{\mathcal{I}}(z)$.

The mean value of the generalized coordinate $X^{\mathcal{I}}(t)$ can be obtained using

$$\langle X^{\mathcal{I}}(t) \rangle = \partial_z \mathcal{G}^{\mathcal{I}}(z, t)|_{z=0} \sim (h^{\mathcal{I}})^{\prime} + t (\lambda_0^{\mathcal{I}})^{\prime} \quad (\text{S16})$$

where Eq.(S15) was used and the prime denotes a partial derivative with respect to z at $z = 0$. The flux of \mathcal{I} -cycle is defined by

$$J_{\mathcal{I}} \equiv \lim_{t \rightarrow \infty} \frac{\langle X^{\mathcal{I}}(t) \rangle}{t} = (\lambda_0^{\mathcal{I}})^{\prime}. \quad (\text{S17})$$

$J_{\mathcal{X}}$ multiplied by the step size d_0 corresponds to the velocity V of motor

Similarly, the diffusion coefficient $D_{\mathcal{I}}$ is obtained by considering the second moment of $X^{\mathcal{I}}$.

$$\begin{aligned} \langle (X^{\mathcal{I}})^2 \rangle &\sim \partial_z^2 \mathcal{G}^{\mathcal{I}}(z, t) \\ &= (h^{\mathcal{I}})^{\prime\prime} + 2t(h^{\mathcal{I}})^{\prime}(\lambda_0^{\mathcal{I}})^{\prime} + t(\lambda_0^{\mathcal{I}})^{\prime\prime} + ((\lambda_0^{\mathcal{I}})^{\prime})^2 t^2, \end{aligned} \quad (\text{S18})$$

which gives

$$D_{\mathcal{I}} = \lim_{t \rightarrow \infty} \frac{\langle (X^{\mathcal{I}}(t))^2 \rangle - \langle X^{\mathcal{I}}(t) \rangle^2}{2t} = \frac{(\lambda_0^{\mathcal{I}})^{\prime\prime}}{2}. \quad (\text{S19})$$

Thus, the diffusion coefficient of motor is obtained: $D = d_0^2 D_{\mathcal{X}}$.

Characteristic polynomial

To express the derivatives of $\lambda_0^{\mathcal{I}}$ in terms of rates $\{k_{ij}\}$, we use the characteristic polynomial of $\Gamma^{\mathcal{I}}(z)$ [1],

$$\det(\lambda_0^{\mathcal{I}} \mathbb{I} - \Gamma^{\mathcal{I}}(z)) = \sum_{n=0}^N (\lambda_0^{\mathcal{I}})^n C_n(z) = 0. \quad (\text{S20})$$

By differentiating both side of Eq.S20 with respect to z and setting $z = 0$, we get

$$C_0' + C_1(\lambda_0^{\mathcal{I}})^{\prime} = 0, \quad (\text{S21})$$

and

$$C_0'' + 2C_1'(\lambda_0^{\mathcal{I}})^{\prime} + C_1(\lambda_0^{\mathcal{I}})^{\prime\prime} + 2C_2((\lambda_0^{\mathcal{I}})^{\prime})^2 = 0. \quad (\text{S22})$$

From Eqs.(S21) and (S22), we get

$$J_{\mathcal{I}} = (\lambda_0^{\mathcal{I}})^{\prime} = -\frac{C_0'}{C_1} \quad (\text{S23})$$

$$D_{\mathcal{I}} = \frac{(\lambda_0^{\mathcal{I}})^{\prime\prime}}{2} = -\frac{C_0'' + 2C_1'(\lambda_0^{\mathcal{I}})^{\prime} + 2C_2(\lambda_0^{\mathcal{I}})^{\prime\prime}}{2C_1} = -\frac{C_0'' + 2J_{\mathcal{I}} + 2C_2 J_{\mathcal{I}}^2}{2C_1} \quad (\text{S24})$$

C_n 's and their derivatives, which depend on the choice

of $X^{\mathcal{I}}$, can readily be found by differentiating the

characteristic polynomial with respect to $\lambda_0^{\mathcal{F}}(z)$ with $\lambda_0^{\mathcal{F}}(0) = 0$ [1].

Explicit expression of $J_{\mathcal{F}}$

The expression of reaction current in each subcycle \mathcal{F} and \mathcal{B} in terms of $\{k_{ij}\}$ can be obtained by considering the corresponding generating function $\mathcal{G}^{\mathcal{I} \in \{\mathcal{F}, \mathcal{B}\}}$. Here, we provide the expression of $J_{\mathcal{F}}$ in terms of rate constants $\{k_{ij}\}$ for the 6-state double-cycle kinetic network.

$$\begin{aligned}
 J_{\mathcal{F}} &= J_{\mathcal{F}}^+ - J_{\mathcal{F}}^- \\
 &= \frac{1}{\Xi} \left(k_{12}(k_{25}k_{32}k_{43} + k_{23}k_{34}k_{45} + k_{25}(k_{32} + k_{34})k_{45})k_{56}k_{61} - k_{16}k_{21}(k_{34}k_{45}k_{52} + k_{32}(k_{43} + k_{45})k_{52} + k_{32}k_{43}k_{54})k_{65} \right)
 \end{aligned} \tag{S25}$$

where

$$\begin{aligned}
 \Xi &= k_{25}k_{32}k_{43} + k_{23}k_{34}k_{45} + k_{25}(k_{32} + k_{34})k_{45} + k_{21}(k_{34}k_{45}(k_{52} + k_{56}) \\
 &+ k_{32}(k_{45}(k_{52} + k_{56}) + k_{43}(k_{52} + k_{54} + k_{56})))k_{61} + k_{21}(k_{34}k_{45}k_{52} + k_{32}(k_{43} + k_{45})k_{52} + k_{32}k_{43}k_{54})k_{65} \\
 &+ k_{16}((k_{25}k_{32}k_{43} + k_{23}k_{34}k_{45} + k_{25}(k_{32} + k_{34})k_{45})k_{56} + (k_{32}k_{43}k_{52} + k_{32}k_{45}k_{52} + k_{34}k_{45}k_{52} + k_{32}k_{43}k_{54}) \\
 &+ k_{25}(k_{34}k_{45} + (k_{34} + k_{43})k_{54} + k_{32}(k_{43} + k_{45} + k_{54})) + k_{23}((k_{43} + k_{45})k_{52} + k_{43}k_{54} + k_{34}(k_{45} + k_{52} + k_{54})))k_{65} \\
 &+ k_{21}(k_{34}k_{45}(k_{52} + k_{56}) + k_{43}k_{54}k_{65} + k_{34}(k_{45} + k_{54})k_{65} + k_{32}(k_{54}k_{65} + k_{45}(k_{52} + k_{56} + k_{65}) \\
 &+ k_{43}(k_{52} + k_{54} + k_{56} + k_{65}))) + k_{12}((k_{34}k_{45}(k_{52} + k_{56}) + k_{32}(k_{45}(k_{52} + k_{56}) + k_{43}(k_{52} + k_{54} + k_{56})))k_{61} \\
 &+ (k_{34}k_{45}k_{52} + k_{32}(k_{43} + k_{45})k_{52} + k_{32}k_{43}k_{54})k_{65} + k_{23}(k_{45}(k_{52} + k_{56})k_{61} \\
 &+ k_{43}(k_{52} + k_{54} + k_{56})k_{61} + k_{45}k_{52}k_{65} + k_{43}(k_{52} + k_{54})k_{65} + k_{34}((k_{52} + k_{54} + k_{56})k_{61} + (k_{52} + k_{54})k_{65} \\
 &+ k_{45}(k_{56} + k_{61} + k_{65}))) + k_{25}(k_{43}k_{54}(k_{61} + k_{65}) + k_{34}(k_{54}(k_{61} + k_{65}) + k_{45}(k_{56} + k_{61} + k_{65})) \\
 &+ k_{32}(k_{54}(k_{61} + k_{65}) + k_{43}(k_{56} + k_{61} + k_{65}) + k_{45}(k_{56} + k_{61} + k_{65}))
 \end{aligned}$$

Similarly, $J_{\mathcal{B}}$ and $D_{\mathcal{X}}$ can also be expressed in terms of $\{k_{ij}\}$.

ANALYSIS OF OTHER TYPES OF KINESINS

Kinesin-1 mutant (Kin6AA)

Single molecule motility data digitized from Ref. [4] was fitted to 6-state network model (Figs. 1A, S4) by using the same method employed for the analysis of kinesin-1 data (**Methods**). However, 4 additional initial conditions for k_{25} ($\{300, 3000, 30000, 300000\}$), thus total 245 initial conditions, were explored. The rate constants estimated from this procedure are provided in Table S2.

Kinesin-2 (KIF17, KIF3AB)

Single molecule motility data digitized from Ref. [5] was again fitted to the 6-state double-cycle kinetic model (Fig. 1A, S6, S8) following the identical procedure employed in the analysis of kinesin-1 data (**Methods**). However, two additional initial conditions for k_{25} ($\{30000, 300000\}$) were explored, which results in total 147 initial conditions. The rate constants are shown in Table S2.

MYOSIN-V

Here we summarize the multi-cyclic model for myosin-V [6] which consists of ATP-dependent chemo-mechanical forward cycle \mathcal{F} , dissipative cycle \mathcal{E} , and ratcheting cycle (ATP independent stepping cycle) \mathcal{M} (Fig. 4A). The \mathcal{E} -cycle, consisting of ATP binding [(2) \rightarrow (5)], ATP hydrolysis [(5) \rightarrow (6)], and ADP

release [(6) \rightarrow (2)] (Figure 4B), was originally introduced to connect the two cycles \mathcal{F} and \mathcal{M} [6]. Calculation of the two currents $J_{\mathcal{E}}$ and $J_{\mathcal{F}}$ reveals that a gradual deactivation of \mathcal{F} -cycle with decreasing [ATP] activates the \mathcal{E} -cycle (Figure S11A, $100 \mu\text{M} \lesssim [\text{ATP}] \lesssim 1 \text{ mM}$, $f \lesssim 1 \text{ pN}$). Thus, \mathcal{E} -cycle can be regarded a futile \mathcal{F} -cycle, which is activated when chemical driving force is balanced with a load f at low [ATP].

We first explain how V and D of myosin-V are calculated, and next express the affinity and heat production (\dot{Q}) in terms of a set of rates $\{k_{ij}\}$. Finally, \mathcal{Q} shall be calculated using V , D , and \dot{Q} .

Calculation of V and D

The \mathcal{M} -cycle consisting of a single state (Fig. 4A) prevents the application of Eq.(S11). To circumvent this difficulty, the model with additional state (5') is considered (Fig. S10). The (5')-state is chemically equivalent to the state (5), but describes motor in different position on actins, such that $X(5) = X_0$ and $X(5') = X_0 \pm d_0$ where $d_0 = 36 \text{ nm}$ for myosin-V. In this new network, the rate constants κ_{ij} 's are

$$\begin{aligned} \kappa_{2,5} &= \kappa_{2,5'} = \frac{k_{25}}{2} \\ \kappa_{6,5} &= \kappa_{6,5'} = \frac{k_{65}}{2} \\ \kappa_{5,2} &= \kappa_{5',2} = k_{52} \\ \kappa_{5,5'}^f &= \kappa_{5',5}^f = k_{55,f} \\ \kappa_{5,5'}^b &= \kappa_{5',5}^b = k_{55,b} \end{aligned} \quad (\text{S26})$$

where the subscripts f and b denote the forward and backward motion, respectively. Other rate constants satisfy $\kappa_{ij} = k_{ij}$. This modification can be justified by considering stochastic movement of myosin-V on the chemical network [7]: $\kappa_{i,5}, \kappa_{i,5'}$ are set to $k_{i5}/2$, such that the outgoing fluxes from the states $i = (2), (6)$ to the state (5) remain identical in the both networks depicted in Fig. 4A and Fig.S10. Next, we set $\kappa_{5,i} = \kappa_{5',i}$ to keep the inward fluxes toward (6), (2) identical for the two networks. Finally, $\kappa_{5,5'}^f = \kappa_{5',5}^f = k_{55,f}$ and $\kappa_{5,5'}^b = \kappa_{5',5}^b = k_{55,b}$. These modification of rate constants enable us to describe transitions within the \mathcal{M} -cycle.

Now, the elements of distance matrix scaled by d_0 are

$$\begin{aligned} d_{3,4}^{\mathcal{X}} &= 1, \\ d_{4,3}^{\mathcal{X}} &= -1, \\ d_{5,5'}^{\mathcal{X},f} &= 1, \\ d_{5',5}^{\mathcal{X},f} &= 1, \\ d_{5,5'}^{\mathcal{X},b} &= -1, \\ d_{5',5}^{\mathcal{X},b} &= -1. \end{aligned} \quad (\text{S27})$$

Other elements ($d_{i,j}^{\mathcal{X}}$) are all zero. Thus, $\Gamma_{i,j}^{\mathcal{X}}$ is written as (with (7) \equiv (5'))

$$\begin{pmatrix} -\kappa_{12}-\kappa_{14} & \kappa_{12} & 0 & \kappa_{14} & 0 & 0 & 0 \\ \kappa_{21} & -\kappa_{21}-\kappa_{23}-\kappa_{25}-\kappa_{26}-\kappa_{27} & \kappa_{23} & 0 & e^z \kappa_{25} & \kappa_{26} & \kappa_{27} \\ 0 & \kappa_{32} & -\kappa_{32}-\kappa_{34} & \kappa_{34} & 0 & 0 & 0 \\ \kappa_{41} & 0 & \kappa_{43} & -\kappa_{41}-\kappa_{43} & 0 & 0 & 0 \\ 0 & e^{-z} \kappa_{52} & 0 & 0 & -\kappa_{52}-\kappa_{56}-\kappa_{57,b}-\kappa_{57,f} & \kappa_{56} & \kappa_{57,b}+\kappa_{57,f} \\ 0 & \kappa_{62} & 0 & 0 & \kappa_{65} & -\kappa_{62}-\kappa_{65}-\kappa_{67} & \kappa_{67} \\ 0 & \kappa_{72} & 0 & 0 & \kappa_{75,b}+\kappa_{75,f} & \kappa_{76} & -\kappa_{72}-\kappa_{75,b}-\kappa_{75,f}-\kappa_{76} \end{pmatrix} \quad (\text{S28})$$

Now, the travel velocity V and the diffusion coefficient D of myosin-V are readily acquired by using Eqs.(S23, S24, and S28). The rate constants used in the calculation are summarized in Table. S4.

Affinities and heat production

The affinities of individual cycles are

$$\begin{aligned} \mathcal{A}_{\mathcal{F}} &= k_B T \log \left(\frac{k_{12} k_{23} k_{34} k_{41}}{k_{21} k_{32} k_{43} k_{41}} \right), \\ \mathcal{A}_{\mathcal{E}} &= k_B T \log \left(\frac{k_{25} k_{56} k_{62}}{k_{52} k_{65} k_{26}} \right), \\ \mathcal{A}_{\mathcal{M}} &= k_B T \log \left(\frac{k_{55,f}}{k_{55,b}} \right). \end{aligned} \quad (\text{S29})$$

Only the following rate constants depend on the load (f):

$$\begin{aligned}
k_{34} &= k_{34}^o e^{-\theta d_m f / k_B T} \\
k_{43} &= k_{43}^o e^{-(1-\theta) d_m f / k_B T} \\
k_{56} &= k_{56}^o \frac{1 + e^{-\chi d_m f_c / k_B T}}{1 + e^{\chi d_m (f - f_c) / k_B T}} \\
k_{52} &= k_{52}^o \frac{1 + e^{-\chi d_m f_c / k_B T}}{1 + e^{\chi d_m (f - f_c) / k_B T}} \\
k_{55,b} &= \frac{D'}{k_B T} \frac{f d_m - U}{d_m^2} \frac{1}{1 - e^{(U - f d_m) / k_B T}} \\
k_{55,f} &= k_{55,b} e^{-f d_m / k_B T}
\end{aligned} \tag{S30}$$

where $\theta = 0.65$, $\chi = 4$, $f_c = 1.6$ pN, $U = 20 k_B T$, $D' = 4.7 \times 10^{-4} \mu\text{m}/\text{s}^2$ as described in Ref. [6]. Thus, the affinities can be written as

$$\begin{aligned}
\mathcal{A}_{\mathcal{F}} &= k_B T \log \left(\frac{k_{12}^o k_{23}^o k_{34}^o k_{41}^o}{k_{21}^o k_{32}^o k_{43}^o k_{41}^o} \right) - f d_0 \\
\mathcal{A}_{\mathcal{E}} &= \mathcal{A}_{\mathcal{E},f=0} \\
\mathcal{A}_{\mathcal{M}} &= -f d_0.
\end{aligned} \tag{S31}$$

The relation $\mathcal{A}_{\mathcal{M}} = -f d_0$ results from the fact that \mathcal{M} -cycle is ATP-independent and activated by the load. Thus, the heat production rate of the system is

$$\dot{Q} = J_{\mathcal{F}} \mathcal{A}_{\mathcal{F}} + J_{\mathcal{E}} \mathcal{A}_{\mathcal{E}} + J_{\mathcal{M}} \mathcal{A}_{\mathcal{M}} \tag{S32}$$

$J_{\mathcal{F}}$, $J_{\mathcal{E}}$, and $J_{\mathcal{M}}$ can be calculated by using Eqs. (S23) and (S28). Finally, \mathcal{Q} for myosin-V is given by

$$\mathcal{Q}_{\text{Myosin-V}} = \dot{Q} \frac{2D}{V^2} \tag{S33}$$

where $D = D_{\mathcal{X}} d_0^2$ and $V = J_{\mathcal{X}} d_0$. S5

DYNEIN

The original model (Figure 5A of Ref. [8]) describes the major pathway of tightly coupled dimeric dynein whose linker connecting the two dynein head domains is short and stiff. This major pathway results from the kinetic simulation of the elastomechanical model [8]. Although the futile cycle, which branches out of the major pathway, is activated at large hindering loads [8], we consider the unicycle model by confining ourselves to the regime of small forces ($f < f_{\text{stall}}$). Thus, only the major forward pathway, where the transitions between the states are denoted by solid black lines in Fig. 5A of Ref. [8], is considered. The model consists of 7 states: dissociation of Pi [(1) \rightarrow (2)]; dissociation of ADP [(2) \rightarrow (3)]; ATP binding [(3) \rightarrow (4)]; dissociation of microtubule binding domain (MTBD) from the

filament [(4) \rightarrow (5)]; power stroke [(5) \rightarrow (6)]; linker swinging to the pre-power stroke state [(6) \rightarrow (7)]; MTBD binding to the filament [(7) \rightarrow (1)]. We also assume only the rate constants describing the mechanical transition of dynein depend on f . The values of rate constants obtained from Ref. [8] are summarized in Table S5. To describe the force-dependence of power-stroke, we model the rate constant for forward and reverse strokes (k_{+PS} and k_{-PS}) as follows.

$$\begin{aligned}
k_{+PS} &= k_{+PS,f=0} e^{-\theta \frac{f d_0}{k_B T}} \\
k_{-PS} &= k_{-PS,f=0} e^{(1-\theta) \frac{f d_0}{k_B T}}
\end{aligned} \tag{S34}$$

where $\theta = 0.3$ is selected based on the previous studies [9, 10]. In the original literature [8], all the rate constants depend on both elastic energy originated from the interaction between two monomer units of dynein, and f . Although this approach will better describe the details of dynein dynamics, it is not possible to calculate elastic energy without explicit simulation of the motion of dyneins which are modeled as elastic materials [8]. Thus, for simplicity, we assume only $k_{\pm PS}$ changes significantly by f . Again, V and D were calculated using Eqs. S23, S24.

Affinity and heat production

The affinity for unicyclic model is written as [11–13]

$$\begin{aligned}
\mathcal{A} &= k_B T \log \prod_{i=1}^N \frac{k_{i,i+1}}{k_{i+1,i}} \\
&= -\Delta\mu_{\text{hyd}} - f d_0
\end{aligned} \tag{S35}$$

where $d_0 = 8.2$ nm. The second term, describing force-dependence, is originated from the use of Eq. S34. Finally, \mathcal{Q} is

$$\mathcal{Q} = \frac{2D}{V d_0} \mathcal{A}. \tag{S36}$$

F₁-ATPASE

Here, we summarize the unicyclic model developed for F₁-ATPase in Ref. [14]. The model is ($N = 2$) unicyclic model (Fig. 4C) where 3 cycles in chemical state space correspond to a single rotation in real space (angle changes by 90° upon transition from the state (1) to state (2) whereas transitions from the state (2) to (1') induce 30° rotation (Fig. 4C). The model is valid when the torque applied to F₁-ATPase is small enough ($\tau \lesssim 30$ pN·nm) that the mechanical cycle is

tightly coupled to the chemical reaction [14]. The dependences of rate constants on the torque are

$$\begin{aligned}
k_{12}(\tau, \zeta) &= k_{12}^{\text{bi}}(\tau, \zeta) \times [\text{ATP}] \\
&= \frac{1}{e^{a_{k_{12}}(\tau)} + \zeta e^{b_{k_{12}}(\tau)}} \times [\text{ATP}] \\
k_{21'}(\tau, \zeta) &= \frac{1}{e^{a_{k_{21'}}(\tau)} + \zeta e^{b_{k_{21'}}(\tau)}} \\
k_{1'2}(\tau, \zeta) &= k_{1'2}^{\text{bi}}(\tau, \zeta) \times [\text{ADP}][\text{Pi}] \\
&= \frac{1}{e^{a_{k_{1'2}}(\tau)} + \zeta e^{b_{k_{1'2}}(\tau)}} \times [\text{ADP}][\text{Pi}] \\
k_{21}(\tau, \zeta) &= \frac{k_{12}(\zeta, \tau) u_2(\zeta, \tau)}{k_{21}(\zeta, \tau)} e^{(\Delta\mu_{\text{hyd}}^0 + \frac{2\pi}{3}\tau)/k_B T} \quad (\text{S37})
\end{aligned}$$

where $\Delta\mu_{\text{hyd}}^0 = -12.5 k_B T \approx -50$ pN·nm, ζ is the friction coefficient (for example, if the γ -shaft of F₁-ATPase is attached to a bead of radius r , $\zeta = 2\pi\eta r^3(4+3\sin^2\pi/6)$ [14] with the water viscosity $\eta = 1$ cP = 10^{-9} pN·s·nm⁻². In our calculation, $r = 40$ nm as in Ref. [14]), and $a_i(\tau), b_i(\tau)$ are polynomial function of τ defined in Ref. [14]. The expressions of $a_i(\tau), b_i(\tau)$ and the coefficients of the polynomials are given in Table. S6.

$V, D, \text{affinities, and heat production}$

For ($N=2$)-unicyclic model, the speed of rotation V , diffusion coefficient D , and affinity \mathcal{A} are [1, 11, 13, 15–18]

$$\begin{aligned}
V &= d_R \frac{k_{1,2}k_{2,1'} - k_{2,1}k_{1',2}}{k_{1,2} + k_{2,1'} + k_{2,1} + k_{1',2}} \equiv d_R J, \\
D &= \frac{d_R^2}{2} \left[\frac{k_{1,2}k_{2,1'}}{k_{2,1}k_{1',2}} + 1 - 2 \left(\frac{k_{1,2}k_{2,1'}}{k_{2,1}k_{1',2}} - 1 \right)^2 \frac{k_{2,1}k_{1',2}}{\sigma^2} \right] \\
&\quad \times \frac{k_{2,1}k_{1',2}}{\sigma}, \\
\mathcal{A} &= k_B T \log \left(\frac{k_{1,2}k_{2,1'}}{k_{2,1}k_{1',2}} \right) \\
&= \left(-\Delta\mu_{\text{hyd}}^0 + k_B T \log \left(\frac{[\text{ATP}]}{[\text{ADP}][\text{P}_i]} \right) \right) - \frac{2\pi}{3}\tau \\
&= -\Delta\mu_{\text{hyd}} - W, \quad (\text{S38})
\end{aligned}$$

where $d_R = \frac{2\pi}{3}$ is the radian distance that motor travels upon ATP hydrolysis, $\sigma = k_{12} + k_{21'} + k_{21} + k_{1'2}$, and $W \equiv \frac{2\pi}{3}\tau$ denotes the work done by the motor. Here, $\tau > 0$ implies the motor performs work against the hindering load. Thus, \mathcal{Q} is given by

$$\mathcal{Q} = \frac{2D}{V d_R} \mathcal{A} \quad (\text{S39})$$

UNICYCLIC KINETIC MODEL FOR KINESIN-1

To analyze the kinesin-1 data, we also considered ($N = 4$)-unicyclic model (Fig. S3A) which was used in our previous study [13]. Briefly, the model consists of four forward rates $\{u_1, u_2, u_3, u_4\}$ and four backward rates $\{w_1, w_2, w_3, w_4\}$. Only $u_1 (= k^{\text{bi}}[\text{ATP}])$ depends on [ATP]. Barometric dependence of the rates on forces are assumed: $u_n = u_n^0 e^{-f d_0 \theta_n^+ / k_B T}$ and $w_n = w_n^0 e^{f d_0 \theta_n^- / k_B T}$ with $\sum_{n=1}^N (\theta_n^+ + \theta_n^-) = 1$ [19, 20]. V, D, \mathcal{A} , and a set of rate constants used in the calculation of \mathcal{Q} are provided in Table. S7 [13].

UNICYCLIC KINETIC MODEL FOR MYOSIN-V

For myosin-V, we also considered the ($N = 2$) unicyclic model from Ref. [21]. Briefly, the model consists of two forward rates $\{u_1, u_2\}$ and two backward rates $\{w_1, w_2\}$. Only $u_1 (= k[\text{ATP}])$ and $w_2 (= k'[\text{ATP}]^\alpha)$ depend on [ATP]. Here, $\alpha = 1/2$. Different choice of α introduces only minor difference in the results as argued in [21]. Barometric dependences of the rates on forces are assumed again: $u_n = u_n^0 e^{-f d_0 \theta_n^+ / k_B T}$ and $w_n = w_n^0 e^{f d_0 \theta_n^- / k_B T}$ with $\sum_{n=1}^N (\theta_n^+ + \theta_n^-) = 1$ [19, 20]. The parameters used in the calculation are available in Eqs. (12), (13) in Ref. [21] and summarized in Table. S8. Identical expressions for V, D , and \mathcal{A} from Eq. S38 were used for the calculation except for $W = f d_0$.

THE LOWER BOUND OF \mathcal{Q} FOR UNICYCLIC MODEL

The analytic expression for the lower bound of the uncertainty measure \mathcal{Q} is available for unicyclic models [22]. For (N)-state unicyclic model, the lower bound of \mathcal{Q} is

$$\mathcal{Q}_b = \frac{\mathcal{A}}{N} \coth \left(\frac{\mathcal{A}}{2N k_B T} \right) \geq 2k_B T. \quad (\text{S40})$$

The \mathcal{Q}_b and the $\Delta\mathcal{Q} \equiv \mathcal{Q} - \mathcal{Q}_b$ of the motors as a function of f and [ATP] are calculated in Figs. S3D (kinesin-1), S14D (F₁-ATPase), and S15D (myosin-V).

* hyeoncb@kias.re.kr

[1] Z. Koza, “General technique of calculating the drift velocity and diffusion coefficient in arbitrary periodic systems,” J. Phys. A. **32**, 7637 (1999).

- [2] A. Wachtel, J. Vollmer, and B. Altaner, “*Fluctuating currents in stochastic thermodynamics. I. Gauge invariance of asymptotic statistics*,” *Phys. Rev. E* **92**, 042132 (2015).
- [3] J. L. Lebowitz and H. Spohn, “*A Gallavotti–Cohen-Type Symmetry in the Large Deviation Functional for Stochastic Dynamics*,” *J. Stat. Phys.* **95**, 333 (1999).
- [4] B. E. Clancy, W. M. Behnke-Parks, J. O. L. Andreasson, S. S. Rosenfeld, and S. M. Block, “*A universal pathway for kinesin stepping*,” *Nat. Struct. Mol. Biol.*
- [5] B. Milic, J. O. L. Andreasson, D. W. Hogan, and S. M. Block, “*Intraflagellar Transport Velocity is Governed by the Number of Active KIF17 and KIF3AB Motors and Their Motility Properties under Load*,” *Proc. Natl. Acad. Sci. U. S. A.* **114**, E6830 (2017).
- [6] V. Bierbaum and R. Lipowsky, “*Chemomechanical Coupling and Motor Cycles of Myosin V*,” *Biophys. J.* **100**, 1747 (2011).
- [7] D. T. Gillespie, “*Exact stochastic simulation of coupled chemical reactions*,” *J. Phys. Chem.*
- [8] A. Šarlah and A. Vilfan, “*The Winch Model Can Explain both Coordinated and Uncoordinated Stepping of Cytoplasmic Dynein*,” *Biophys. J.* **107**, 662 (2014).
- [9] M. P. Singh, R. Mallik, S. P. Gross, and C. C. Yu, “*Monte carlo modeling of single-molecule cytoplasmic dynein*,” *Proc. Natl. Acad. Sci.* **102**, 12059 (2005).
- [10] J. A. Wagoner and K. A. Dill, “*Molecular motors: Power strokes outperform brownian ratchets*,” *J. Phys. Chem. B* **120**, 6327 (2016).
- [11] H. Qian and D. A. Beard, “*Thermodynamics of Stochastic Biochemical Networks in Living Systems Far From Equilibrium*,” *Biophys. Chem.* **114**, 213 (2005).
- [12] U. Seifert, “*Entropy production along a stochastic trajectory and an integral fluctuation theorem*,” *Phys. Rev. Lett.* **95**, 040602 (2005).
- [13] W. Hwang and C. Hyeon, “*Quantifying the heat dissipation from molecular motor’s transport properties in nonequilibrium steady states*,” *J. Phys. Chem. Lett.* **8**, 250 (2017).
- [14] E. Gersitsma and P. Gaspard, “*Chemomechanical coupling and stochastic thermodynamics of the F1-ATPase molecular motor with an applied external torque*,” *Biophys. Rev. Lett.* **05**, 163 (2010).
- [15] B. Derrida, “*Velocity and diffusion constant of a periodic one-dimensional hopping model*,” *J. Stat. Phys.* **31**, 433 (1983).
- [16] M. E. Fisher and A. B. Kolomeisky, “*The force exerted by a molecular motor*,” *Proc. Natl. Acad. Sci.* **96**, 6597 (1999).
- [17] H. Qian, “*Phosphorylation energy hypothesis: Open chemical systems and their biological functions*,” *Annu. Rev. Phys. Chem.* **58**, 113 (2007).
- [18] U. Seifert, “*Stochastic Thermodynamics, Fluctuation Theorems and Molecular Machines*,” *Rep. Prog. Phys.* **75**, 126001 (2012).
- [19] M. E. Fisher and A. B. Kolomeisky, “*The force exerted by a molecular motor*,” *Proc. Natl. Acad. Sci. U. S. A.* **96**, 6597 (1999).
- [20] M. E. Fisher and A. B. Kolomeisky, “*Simple mechanochemistry describes the dynamics of kinesin molecules*,” *Proc. Natl. Acad. Sci. U. S. A.* **98**, 7748 (2001).
- [21] A. B. Kolomeisky and M. E. Fisher, “*A Simple Kinetic Model Describes the Processivity of Myosin-V*,” *Biophys. J.* **84**, 1642 (2003).
- [22] A. C. Barato and U. Seifert, “*Thermodynamic Uncertainty Relation for Biomolecular Processes*,” *Phys. Rev. Lett.* **114**, 158101 (2015).
- [23] K. Visscher, M. J. Schnitzer, and S. M. Block, “*Single Kinesin Molecules Studied with a Molecular Force Clamp*,” *Nature* **400**, 184 (1999).
- [24] S. Liepelt and R. Lipowsky, “*Kinesin’s Network of Chemomechanical Motor Cycles*,” *Phys. Rev. Lett.* **98**, 258102 (2007).

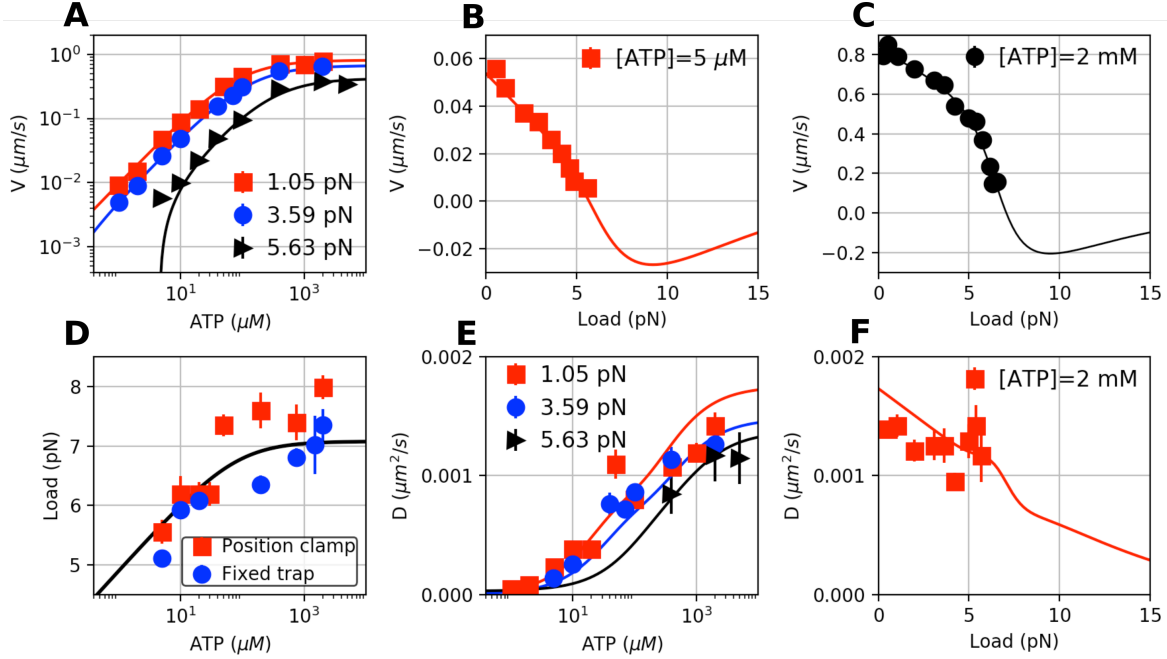


FIG. S1. Analysis of experimental data of kinesin-1, digitized from Ref. [23], using the 6-state model [24]. The solid lines are the fits to the data **A**. V vs [ATP] at $f=1.05$ pN (red square), 3.59 pN (blue circle), and 5.63 pN (black triangle). **B**. V vs f at [ATP] = 5 μM . **C**. V vs f at [ATP] = 2 mM. **D**. Stall force as a function of [ATP], measured by ‘Position clamp’ (red square) or ‘Fixed trap’ (blue circle) methods. **E**. D vs [ATP] at $f=1.05$ pN (red square), 3.59 pN (blue circle), and 5.63 pN (black triangle). D was estimated from $r = 2D/Vd_0$. **F**. D vs f at [ATP] = 2 mM.

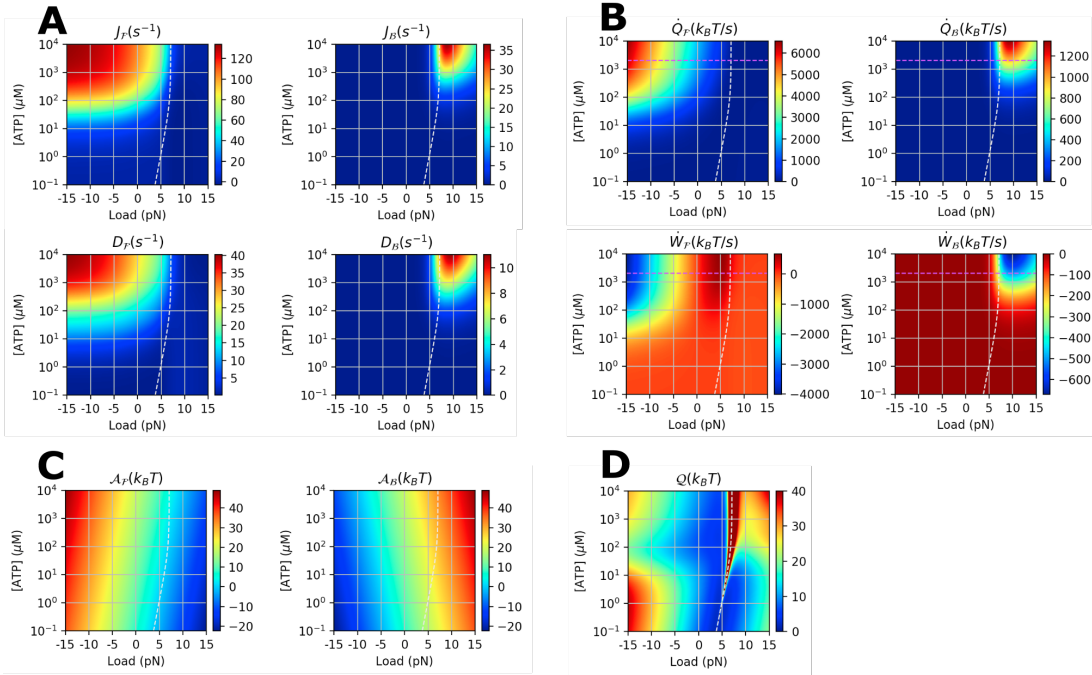


FIG. S2. Various physical properties of kinesin-1 calculated using the 6-state network model (Fig. 1A) at varying f and [ATP]. **A**. Transport properties (flux J and D). **B**. Heat \dot{Q} and work production \dot{W} . **C**. Thermodynamic affinity \mathcal{A} . **D**. $Q(f, [\text{ATP}])$. The white dashed lines indicate the stall condition.

(N=4)-uni cyclic

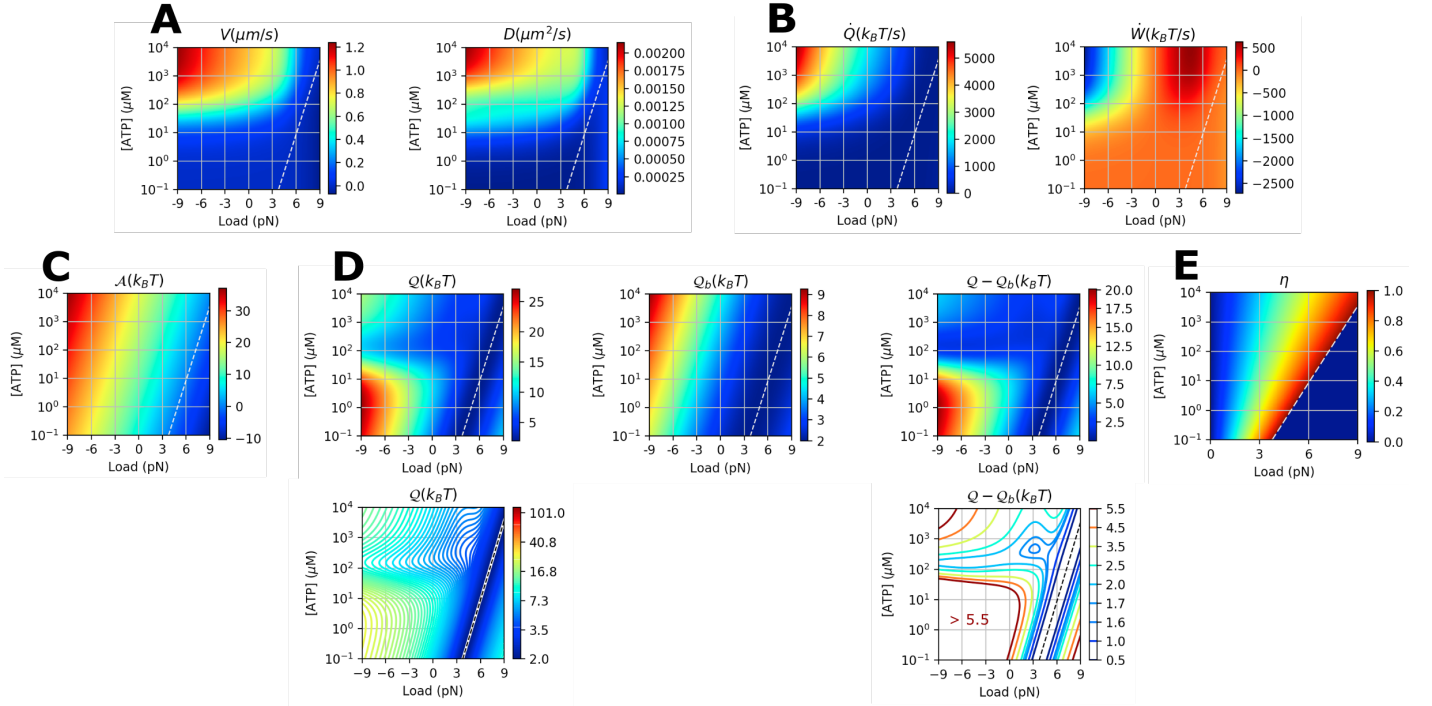
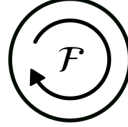


FIG. S3. Various physical properties of kinesin-1 calculated using (N=4)-uni cyclic model [13, 20] at varying f and [ATP]. We used the same model parameters from Ref. [13]. **A.** Transport properties (V , D). **B.** Heat \dot{Q} and work production \dot{W} . **C.** Thermodynamic affinity \mathcal{A} . **D.** Q , Q_b (Eq.S40), and their difference $\Delta Q = Q - Q_b$. For clarity, identical data of Q and ΔQ are shown again using contour plots. **E.** Power efficiency $\eta \equiv \dot{W}/(\dot{W} + \dot{Q})$ ($\eta = 0$ for $f > f_{\text{stall}}$). The white dashed lines indicate the stall condition.

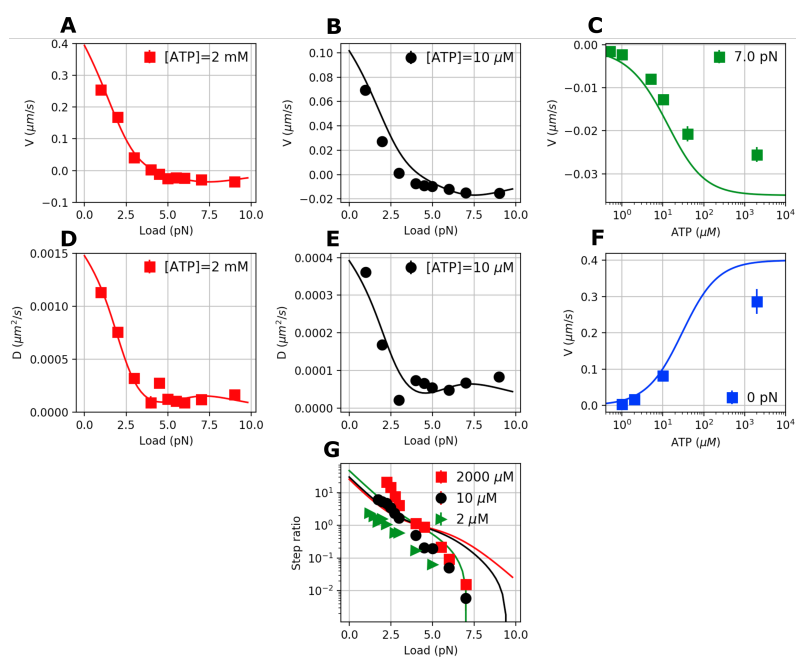


FIG. S4. Motility data of Kin6AA, a mutant made of kinesin-1 to which six additional amino-acids are inserted in the neck-linker domains [4], and the theoretical fits made using the 6-state double-cycle kinetic network model (Fig. 1A).

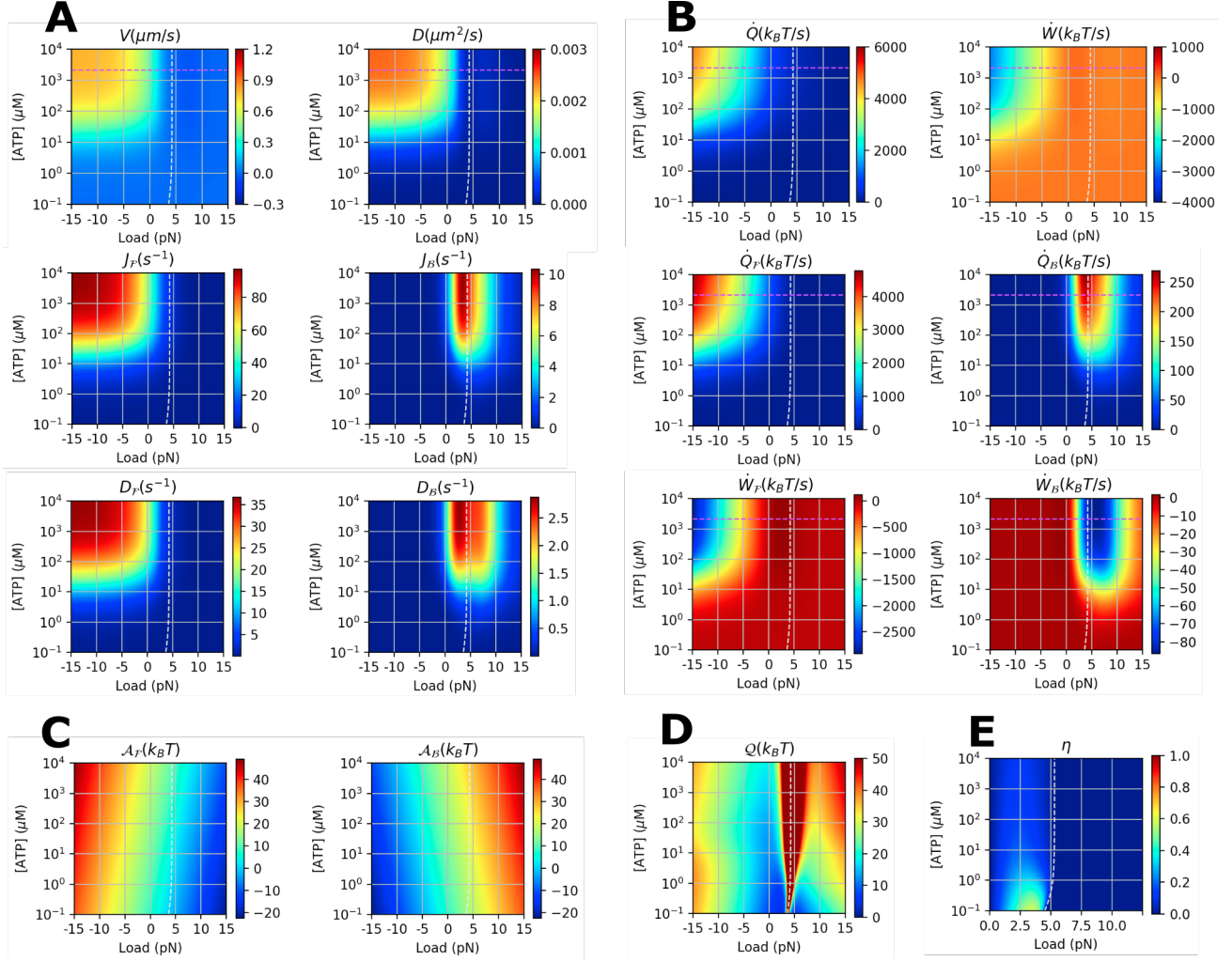


FIG. S5. Various physical properties of kin6AA calculated using 6-state network model (Fig. 1A) at varying f and $[ATP]$. **A.** Transport properties (J , D). **B.** Heat \dot{Q} and work production \dot{W} . **C.** Thermodynamic affinity \mathcal{A} . **D.** $Q(f, [ATP])$. **E.** Power efficiency $\eta \equiv \dot{W}/(\dot{W} + \dot{Q})$ ($\eta = 0$ for $f > f_{\text{stall}}$). The white dashed lines indicate the stall condition.

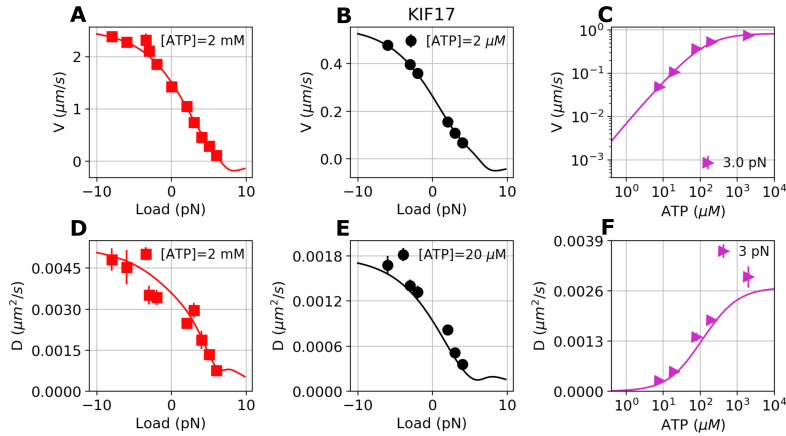


FIG. S6. Motility data of homodimeric kinesin-2 (KIF17) [5] and their theoretical fits (solid lines).

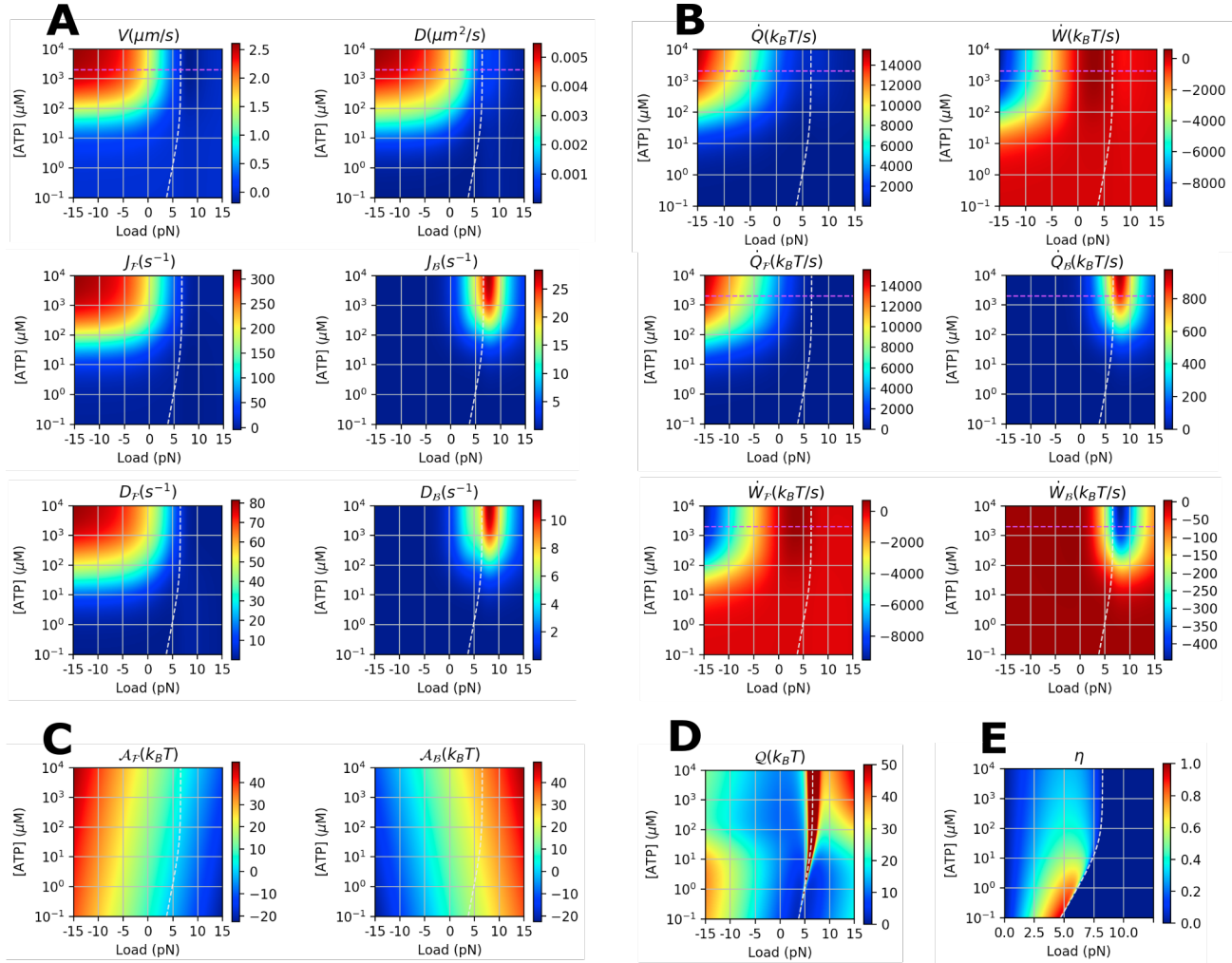


FIG. S7. Various physical properties of KIF17 calculated using 6-state network model (Fig. 1A) at varying f and $[ATP]$. **A.** Transport properties (J , D). **B.** Heat \dot{Q} and work production \dot{W} . **C.** Thermodynamic affinity \mathcal{A} . **D.** $Q(f, [ATP])$. **E.** Power efficiency $\eta \equiv \dot{W}/(\dot{W} + \dot{Q})$ ($\eta = 0$ for $f > f_{\text{stall}}$). The white dashed lines indicate the stall condition.

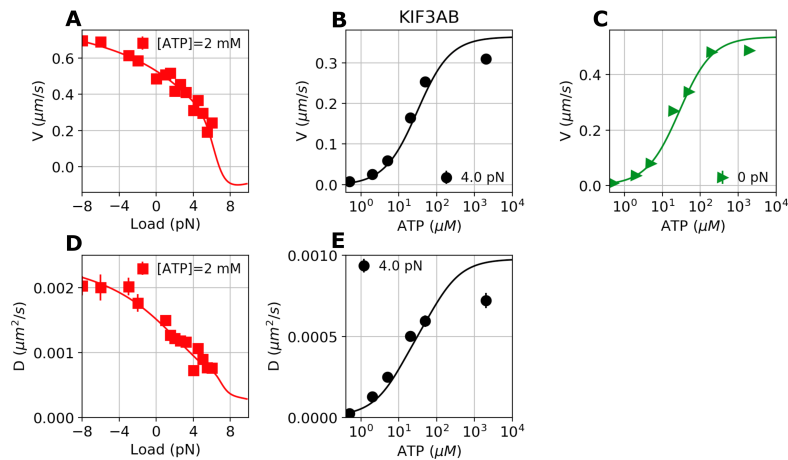


FIG. S8. Motility data of heterotrimeric kinesin-2 (KIF3AB) [5] and their theoretical fits (solid lines).

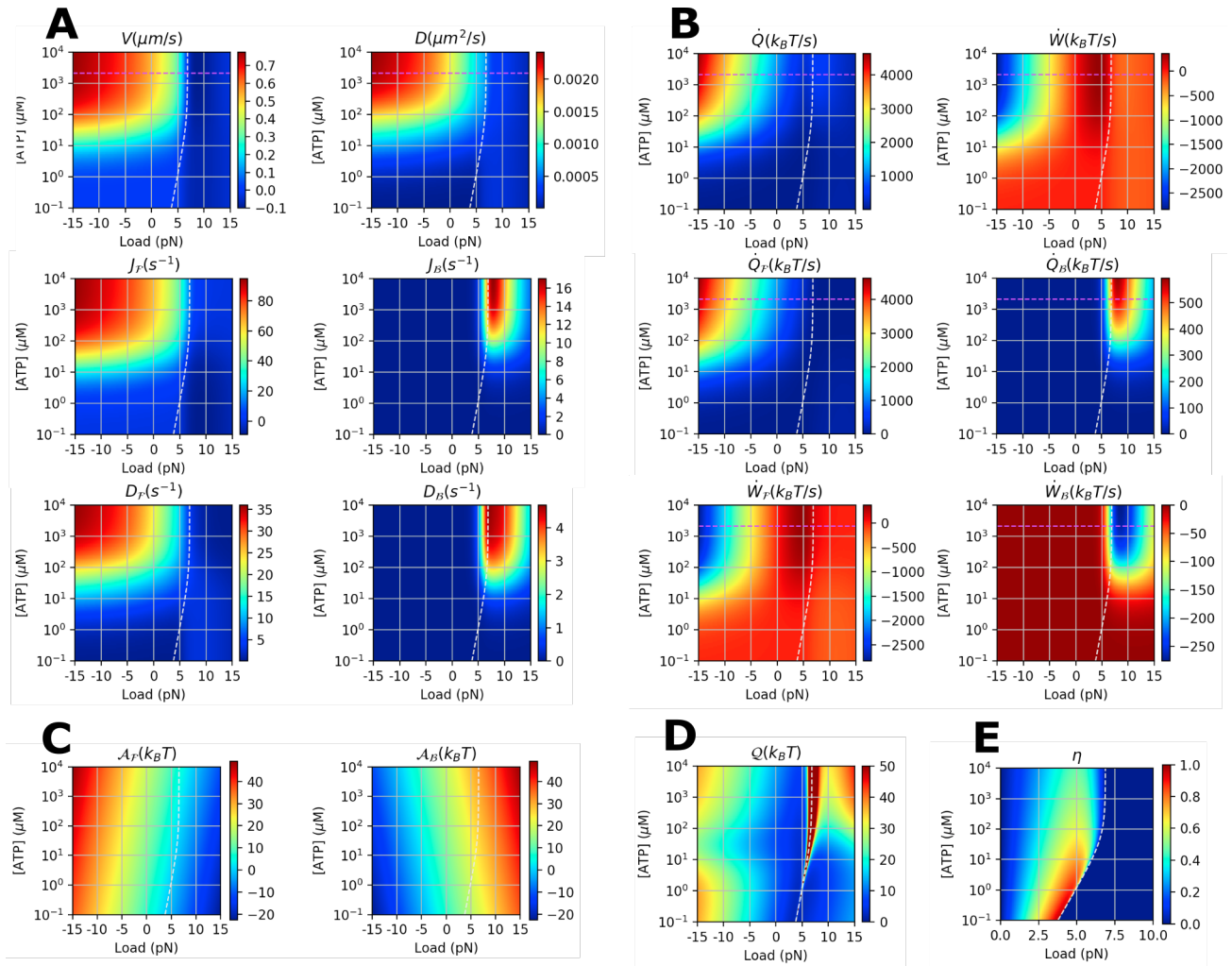


FIG. S9. Various physical properties of KIF3AB calculated using the 6-state network model (Fig. 1A) at varying f and $[ATP]$. **A.** Transport properties (J , D). **B.** Heat \dot{Q} and work production \dot{W} . **C.** Thermodynamic affinity \mathcal{A} . **D.** $Q(f, [ATP])$. **E.** Power efficiency $\eta \equiv \dot{W}/(\dot{W} + \dot{Q})$ ($\eta = 0$ for $f > f_{\text{stall}}$). The white dashed lines indicate the stall condition.

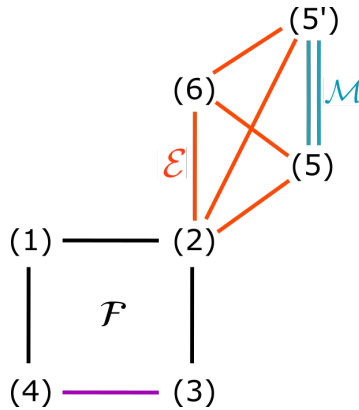


FIG. S10. Augmented kinetic network model of myosin-V. Each line represents a reversible kinetics.

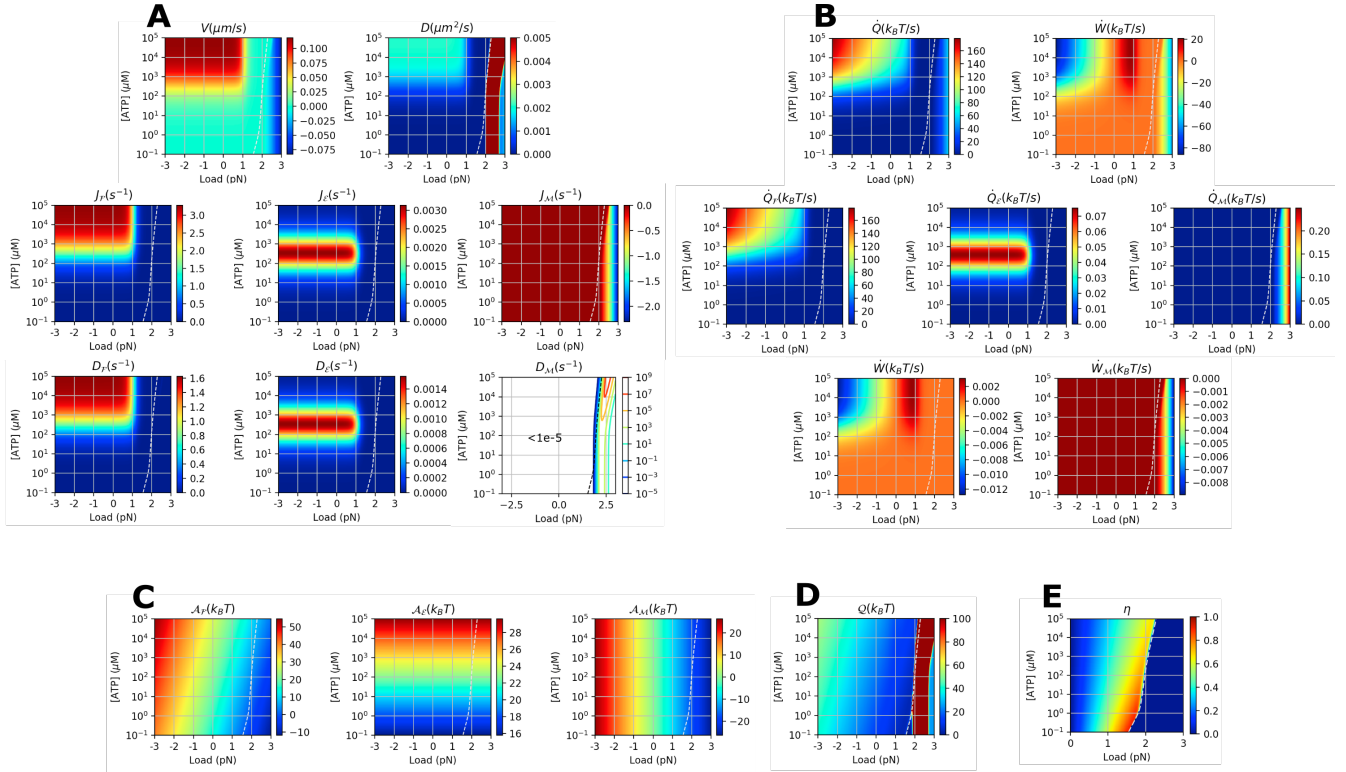


FIG. S11. Various physical properties of myosin-V calculated using the multi-cyclic model [6] at varying f and $[\text{ATP}]$. $[\text{ADP}] = 70 \mu\text{M}$ and $[\text{Pi}] = 1 \text{ mM}$ condition was used for the calculation. **A.** Transport properties (J , D). **B.** Heat \dot{Q} and work production \dot{W} . **C.** Thermodynamic affinity \mathcal{A} . **D.** $Q(f, [\text{ATP}])$. **E.** Power efficiency $\eta \equiv \dot{W}/(\dot{W} + \dot{Q})$ ($\eta = 0$ for $f > f_{\text{stall}}$). The white dashed lines indicate the stall condition.

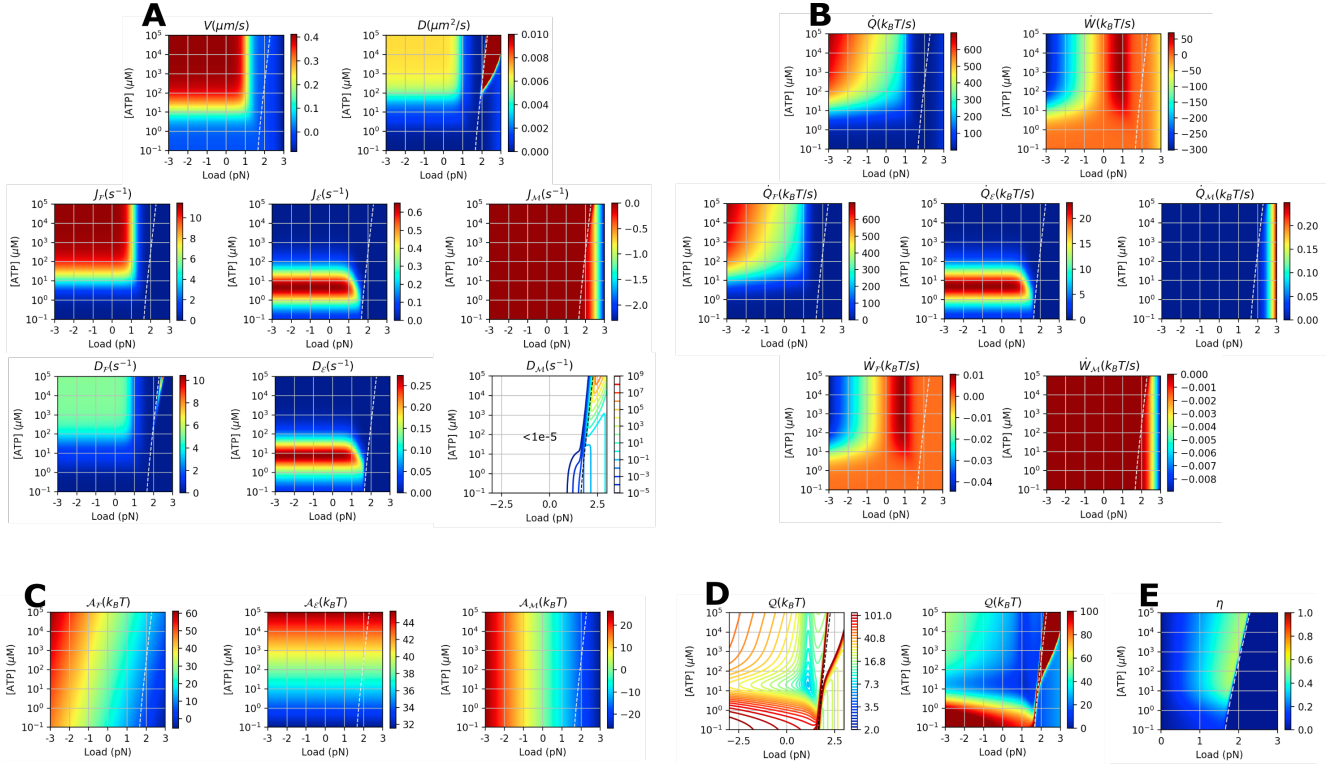


FIG. S12. Various physical properties of myosin-V calculated using the multi-cyclic model [6] at varying f and $[ATP]$. $[ADP] = 0.1 \mu M$ and $[Pi] = 0.1 \mu M$ condition was used for the calculation. **A.** Transport properties (J , D). **B.** Heat \dot{Q} and work production \dot{W} . **C.** Thermodynamic affinity \mathcal{A} . **D.** $\mathcal{Q}(f, [ATP])$. **E.** Power efficiency $\eta \equiv \dot{W}/(\dot{W} + \dot{Q})$ ($\eta = 0$ for $f > f_{stall}$). The white dashed lines indicate the stall condition.

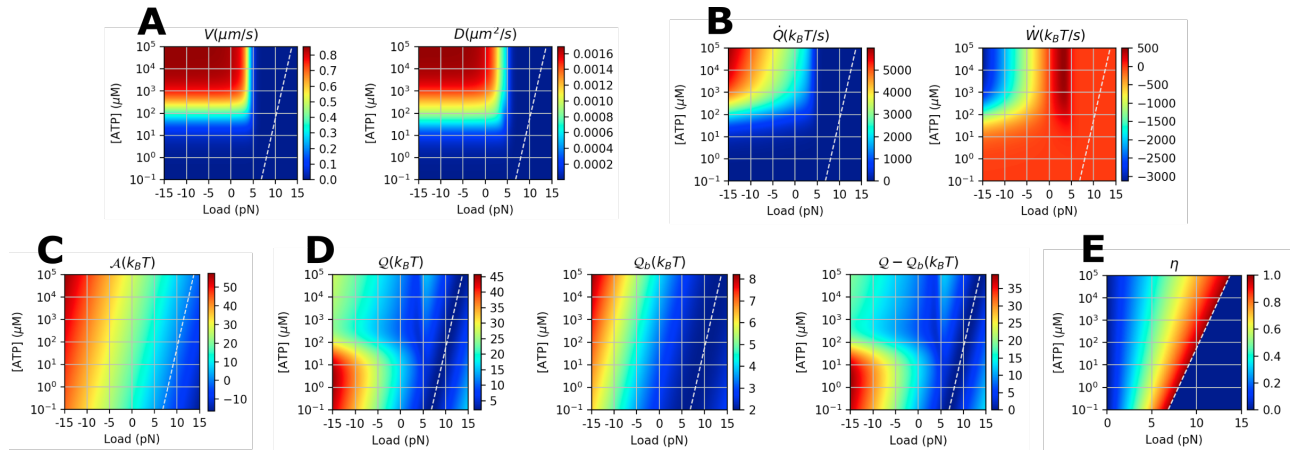


FIG. S13. Various physical properties of dynein monomer calculated using the $(N = 7)$ -unicyclic model [8] at varying f and $[ATP]$. $[ADP] = 70 \mu M$ and $[Pi] = 1 mM$ condition was used for the calculation. **A.** Transport properties (V , D). **B.** Heat \dot{Q} and work production \dot{W} . **C.** Thermodynamic affinity \mathcal{A} . **D.** $\mathcal{Q}(f, [ATP])$, $\mathcal{Q}_b(f, [ATP])$, and $\Delta \mathcal{Q}(f, [ATP])$. **E.** Power efficiency $\eta \equiv \dot{W}/(\dot{W} + \dot{Q})$ ($\eta = 0$ for $f > f_{stall}$). The white dashed lines indicate the stall condition.

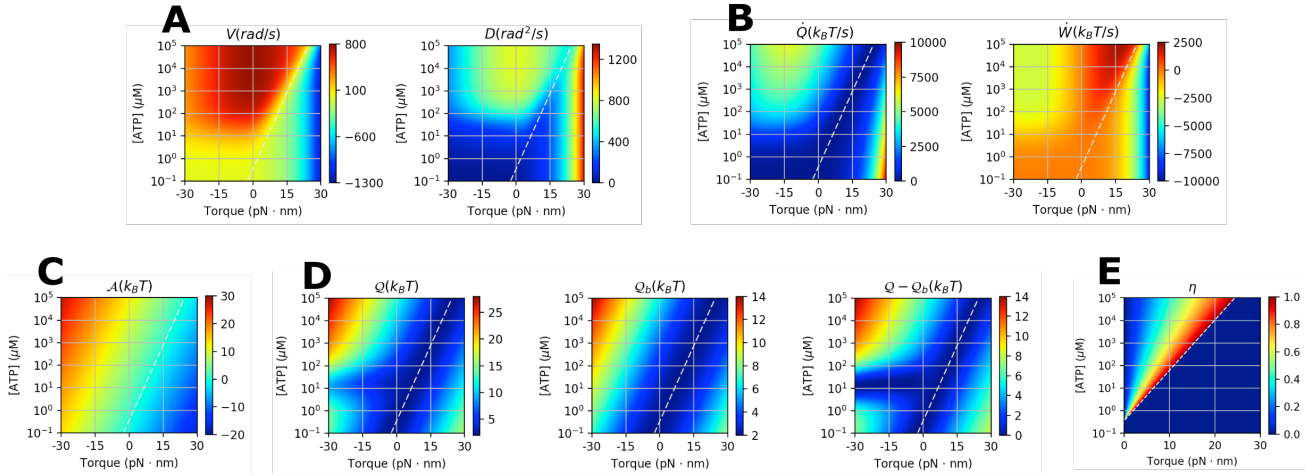


FIG. S14. Various physical properties of F_1 -ATPase calculated using ($N = 2$)-unicyclic model (Fig. 4C) at varying f and $[ATP]$. $[ADP] = 70 \mu M$ and $[Pi] = 1 mM$ condition was used for the calculation. **A.** Transport properties (V , D). **B.** Heat \dot{Q} and work production \dot{W} . **C.** Thermodynamic affinity \mathcal{A} . **D.** Q , Q_b (Eq.S40), and their difference $\Delta Q = Q - Q_b$. **E.** Power efficiency $\eta \equiv \dot{W}/(\dot{W} + \dot{Q})$ ($\eta = 0$ for $f > f_{stall}$). The white dashed lines indicate the stall condition.

(N=2)-uni cyclic

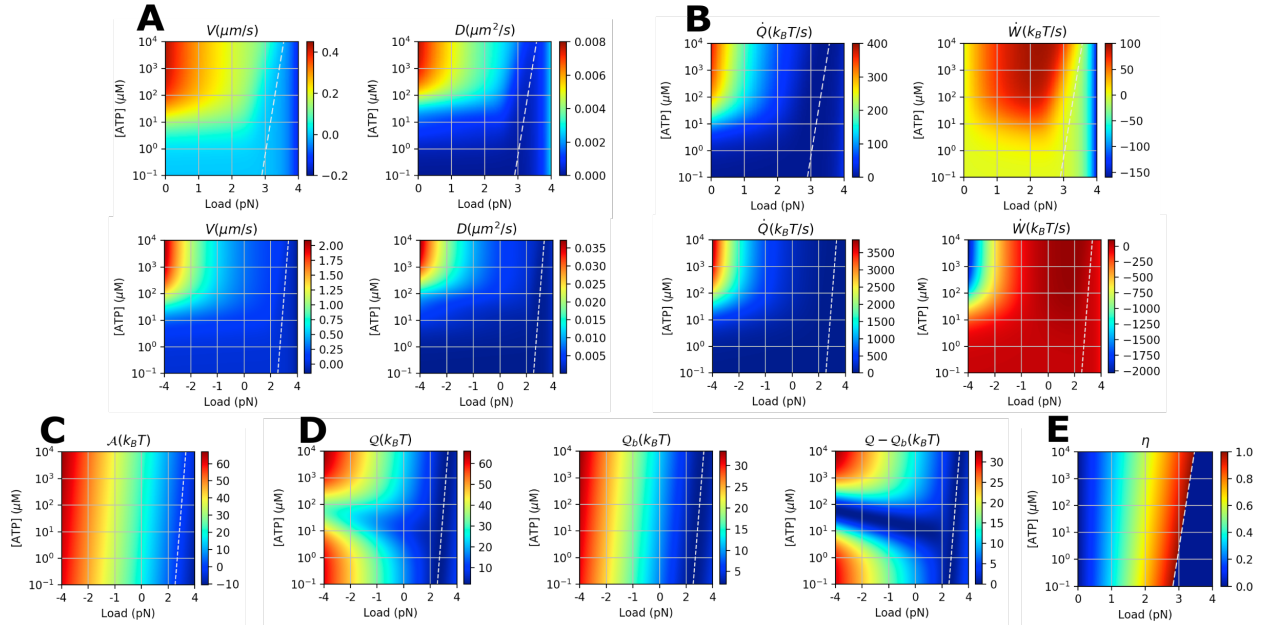
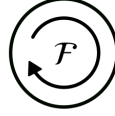


FIG. S15. Various physical properties of myosin-V calculated using ($N = 2$)-unicyclic model [21] at varying f and $[ATP]$. **A.** Transport properties (V , D). Same data are shown twice over the different range of f for clarity. **B.** Heat \dot{Q} and work production \dot{W} . Same data are shown twice over the different range of f for clarity. **C.** Thermodynamic affinity \mathcal{A} . **D.** Q , Q_b (Eq.S40), and their difference $\Delta Q = Q - Q_b$. **E.** Power efficiency $\eta \equiv \dot{W}/(\dot{W} + \dot{Q})$ ($\eta = 0$ for $f > f_{stall}$). The white dashed lines indicate the stall condition.

TABLE S1. Optimal f and $[ATP]$ that locally minimize \mathcal{Q} . For unicyclic models of kinesin-1, myosin-V, and F₁-ATPase, also shown are f and $[ATP]$ that minimizes $\Delta\mathcal{Q} = \mathcal{Q} - \mathcal{Q}_b$, where \mathcal{Q}_b is a stronger lower bound for unicyclic kinetic schemes [22] (Eq.S40).

	Kinesin-1 (multi-cycle)	Kinesin-1 (unicycle)	KIF17 (multi-cycle)	Myosin-V (multi-cycle) [ADP]=[P _i]=0.1 μM	Myosin-V (unicycle)	Dynein (unicycle)	F ₁ -ATPase (unicyclic)
f (pN)	4.1	3.2 ^a	1.5	1.1	0.03 ^a	3.9	8.6 ^{a b}
$[ATP]$ (μM)	210	460 ^a	200	20	17 ^a	200	16 ^a
\mathcal{Q}_{\min} ($k_B T$)	4.0	4.5	9.2	6.5	14	5.2	4.2
$\Delta\mathcal{Q}_{\min}$ ($k_B T$)	n/a	1.6	n/a	n/a	0	2.6	0

^a Condition for local minimization of $\Delta\mathcal{Q} = \mathcal{Q} - \mathcal{Q}_b$.

^b For F₁-ATPase, we consider a resisting torque (τ with the unit of pN·nm) against the rotation of the motor.

TABLE S2. Parameters determined for the 6-state double-cycle model [24]. The unit of rate constants ($\{k_{ij}\}$) is s^{-1} except for k_{ij}^{bi} ($[k_{ij}^{bi}] = \mu M^{-1} s^{-1}$). The rates in the table are determined for $f = 0$.

	Kinesin-1	Kin6AA	KIF17	KIF3AB
k_{12}^{bi}	2.8	10	10	10
k_{21}	4200	92	3600	500
k_{25}	1.6×10^6	1.6×10^4	4.0×10^4	6.2×10^6
k_{52}	1.1	3.4	0.079	7.2
k_{56}	190	680	590	92
k_{65}	10	4.1	13	37
k_{61}	250	58	310	320
k_{16}	230	260	1100	750
k_{54}	2.1×10^{-9}	4.3×10^{-6}	1.4×10^{-8}	6.8×10^{-10}
θ	0.61	0.59	0.34	0.82
χ_{12}	0.15	0.12	0.15	0.09
χ_{56}	0.0015	0.0	0.012	0.021
χ_{61}	0.11	0.18	0.17	0.16

TABLE S3. Initial values and constraints applied during the fit of kinesin data using 6-state double-cyclic model. The units are identical to those in Table S2. For k_{65} and k_{16} , we used 7 initial values (0.001, 0.01, 0.1, 1, 10, 100, 1000) for the fits.

k_{12}^{bi}	$0.5 \leq 1.8 \leq 10$	k_{56}	$10 \leq 200 \leq 10^4$	k_{61}	$10 \leq 200 \leq 10^4$	k_{25}	$10^4 \leq 3 \times 10^5 \leq 10^7$
k_{21}	$10 \leq 100 \leq 10^4$	k_{65}	$10^{-4} \leq 10^{[-3,-2,-1,0,1,2,3]} \leq 10^4$	k_{16}	$0^{-4} \leq 10^{[-3,-2,-1,0,1,2,3]} \leq 10^4$		
θ	$0 \leq 0.3 \leq 1$	χ_{12}	$0 \leq 0.25 \leq 1$	χ_{56}	$0 \leq 0.05 \leq 1$	χ_{61}	$0 \leq 0.05 \leq 1$

TABLE S4. Parameters used for calculation of \mathcal{Q} of myosin-V. The values are obtained from Ref. [6]. The unit of rate constants ($\{k_{ij}\}$) is s^{-1} except for k_{ij}^{bi} ($[k_{ij}^{bi}] = \mu M^{-1} s^{-1}$). The rates in the table are determined for $f = 0$.

	Description	value
k_{12}	ADP release	1.2
k_{21}^{bi}	ADP binding	4.5
k_{23}^{bi}	ATP binding	0.9
k_{32}	ATP release	2×10^{-5}
k_{34}	step	7000
k_{43}	reverse step	0.65
k_{56}^{bi}	ATP binding	0.9
k_{65}	ATP release	2×10^{-5}
$k_{55,f}$	step (mechanical)	1.5×10^{-8}
$k_{55,b}$	reverse step (mechanical)	1.5×10^{-8}

TABLE S5. Parameters used for calculation of \mathcal{Q} of dynein. The values are obtained from Table 3. of Ref. [8]. The unit of rate constants ($\{k_{ij}\}$) is s^{-1} except for k_{ij}^{bi} ($[k_{ij}^{bi}] = \mu M^{-1} s^{-1}$). The rates in the table are determined for $f = 0$.

	Description	value
k_{12}	Pi release	5000
k_{21}^{bi}	Pi binding	0.01
k_{23}	ADP release	160
k_{32}^{bi}	ADP binding	2.7
k_{34}^{bi}	ATP binding	2
k_{43}	ATP release	50
k_{45}	MT release in poststroke state	500
k_{54}	MT binding in poststroke state	100
k_{56}	Power stroke	5000
k_{65}	Reverse stroke	10
k_{67}	linker swing to prestroke	1000
k_{76}	linker swing to poststroke	100
k_{71}	MT binding in prestroke state	10000
k_{17}	MT release in prestroke state	500

TABLE S6. Polynomial coefficient of $a_i(\tau) = a_i^{(0)} + a_i^{(1)}\tau + a_i^{(2)}\tau^2$ and $b_i(\tau) = b_i^{(0)} + b_i^{(1)}\tau + b_i^{(2)}\tau^2$ used in F₁-ATPase ($N = 2$)-unicyclic model. The values are obtained from Table 3. of Ref. [14].

	$i = k_{12}$	$i = k_{21'}$	$i = k_{1'2}$	Unit
$a_i^{(0)}$	-16.952	-5.973	-19.382	-
$a_i^{(1)}$	9.8×10^{-4}	1.7×10^{-4}	0.129	(pN nm) ⁻¹
$a_i^{(2)}$	5.8×10^{-4}	1.0×10^{-3}	2.8×10^{-4}	(pN nm) ⁻²
$b_i^{(0)}$	-16.352	-2.960	-18.338	-
$b_i^{(1)}$	-6.6×10^{-2}	-2.7×10^{-2}	5.9×10^{-3}	(pN nm) ⁻¹
$b_i^{(2)}$	1.0×10^{-3}	3.6×10^{-4}	-2.1×10^{-4}	(pN nm) ⁻²

TABLE S7. Parameters of (N=4)-unicyclic model of kinesin-1. The values are obtained from our previous study [13]. The unit of $\{u_n\}$ and $\{w_n\}$ is s^{-1} except for u_1^o ($[u_1^o] = \mu M^{-1} s^{-1}$).

u_1^o	2.3	u_2	600	u_3	400	u_4	190
θ_1^+	0.00	θ_2^+	0.04	θ_3^+	0.01	θ_4^+	0.02
w_1	20	w_2	1.4	w_3	1.7	w_4	120
θ_1^-	0.14	θ_2^-	0.15	θ_3^-	0.5	θ_4^-	0.14

TABLE S8. Parameters for ($N = 2$)-unicyclic model of myosin-V. The values are obtained from Eqs. (12), (13) in Ref. [21]. The unit of rate constants ($\{u_i, w_i\}$) is s^{-1} except for k and k' ($[k, k'] = \mu M^{-1} s^{-1}$). The rates in the table are determined for $f = 0$.

k	0.70
w_1	6×10^{-6}
u_2	12
k'	5.0×10^{-6}
θ_1^+	-0.01
θ_1^-	0.045
θ_2^+	0.385
θ_2^-	0.58